Materials and Design 89 (2016) 715–720

Contents lists available at ScienceDirect

Materials and Design

journal homepage: www.elsevier.com/locate/jmad

Effect of oxygen vacancies on structural, electrical and magnetic properties of $La_{0.67}Sr_{0.33}CoO_3$ thin films

Bin Liu [a,b], Guiju Liu [a,b], Honglei Feng [a,b], Chao Wang [a,b], Huaiwen Yang [c,d], Yiqian Wang [a,b,*]

[a] College of Physics, Qingdao University, No. 308, Ningxia Road, Qingdao 266071, People's Republic of China
[b] The Cultivation Base for State Key Laboratory, Qingdao University, No. 308, Ningxia Road, Qingdao 266071, People's Republic of China
[c] State Key Laboratory of Magnetism, Institute of Physics, Chinese Academy of Sciences, Beijing 100080, People's Republic of China
[d] Beijing National Laboratory for Condensed Matter Physics, Institute of Physics, Chinese Academy of Sciences, Beijing 100080, People's Republic of China

ARTICLE INFO

Article history:
Received 4 July 2015
Received in revised form 14 September 2015
Accepted 8 October 2015
Available online 13 October 2015

Keywords:
$La_{0.67}Sr_{0.33}CoO_3$ thin film
Modulated structure
Anisotropic chemical expansion
Metal–insulator transition

ABSTRACT

The microstructure and chemical expansion of annealed and unannealed $La_{0.67}Sr_{0.33}CoO_3$ (LSCO) thin films were investigated using high-resolution transmission electron microscopy (HRTEM). In both annealed and unannealed LSCO thin films, the modulated structure in La/Sr planes (A-sites) was discovered, which is ascribed to the cation ordering. However, the oxygen vacancy ordering induced modulated structure in Co–O planes (B-sites) only appeared in the vacuum-annealed LSCO thin films. In addition, the anisotropic chemical expansion was only observed in the vacuum-annealed LSCO films and the anisotropic elongation is associated with the modulated structures in the Co–O planes. What's more, the electrical and magnetic properties of the LSCO thin films were studied before and after annealing in the vacuum. The ferromagnetic-metallic LSCO thin films turned into a non-magnetic insulator after the annealing in vacuum, which is attributed to appearance of the oxygen vacancy ordering in the vacuum-annealed LSCO films.

1. Introduction

$LaCoO_3$-based perovskite oxide materials have been widely studied, and a variety of modulated structures have been observed [1–6], particularly after doping with alkaline earth metals such as Sr, Pr, and Cr. However, the formation mechanism of these modulated structures is still inconclusive. According to the previous reports [1–6], the modulated structures could result from cation ordering, spin ordering or oxygen vacancy ordering. Wang et al. [1] found that the $La_{0.5}Sr_{0.5}CoO_3$ and $La_{0.33}Sr_{0.67}CoO_3$ films have a modulated structure with a periodicity of two-fold and three-fold the original unit lattice, respectively, and they believed that the modulated structures are induced by cation ordering. While other researchers thought that the emergence of the modulated stripes is associated with the spin ordering [2,3] or oxygen vacancy ordering [4–6]. To our best knowledge, no report has provided a direct evidence to prove that the cation ordering and oxygen vacancy ordering can coexist in the $LaCoO_3$-based perovskite thin film.

Recently, thermal and chemical expansions in $LaCoO_3$-based perovskite films have been investigated by in-situ high-temperature X-ray diffraction (XRD) [7–11]. It is concluded that the chemical expansion was caused by the reduction of oxidation state of Co^{4+} and the anisotropic expansion was significantly larger along *c*-axis relative to *a*-axis. However, all the data were obtained by XRD and no direct evidence was shown to verify the anisotropic elongation. Besides, the exact origin of the anisotropic chemical expansion of LSCO films has not yet been unveiled. In our work, the anisotropic chemical expansion was directly observed in the vacuum-annealed LSCO films using high-resolution transmission electron microscopy (HRTEM). More importantly, we found that the anisotropic chemical expansion is associated with the modulated structures in the vacuum-annealed LSCO film.

The ferromagnetism and conductivity of $LaCoO_3$-based perovskite oxides have received considerable attention due to their potential applications in ferroelectric memory, solid-oxide fuel cells, mixed ionic and electronic conducting membranes [6,12]. It was demonstrated that the ferromagnetism and conductivity of the $LaCoO_3$-based oxides are originated from the double-exchange interaction between the Co–O–Co bonds [13–15]. In our work, the magnetic and electrical properties of unannealed and vacuum-annealed LSCO films were compared and correlated with their microstructures.

2. Experimental details

The 30-nm-thick $La_{0.67}Sr_{0.33}CoO_3$ (LSCO) film was epitaxially grown on (001) $SrTiO_3$ (STO) substrate using a single-target pulsed laser deposition (PLD) technique. The target for the PLD system was made from ceramic powders prepared using a mixed oxide sintering method. The laser wavelength is 248 nm, the pulse energy is 1.5 J/cm^2, and the sputtering frequency is 1 Hz. During the sputtering process, the substrate is maintained at 750 °C and the oxygen partial pressure is 50 Pa.

* Corresponding author.
E-mail address: yqwang@qdu.edu.cn (Y. Wang).

http://dx.doi.org/10.1016/j.matdes.2015.10.034
0264-1275/

After the sputtering process, the film is kept at 90 Pa for 15 min, and then cooled down to room temperature naturally. During the annealing process, the film is maintained at 300 °C for 1 min at 10^{-4} Pa, and then cooled down to room temperature slowly.

The specimens for transmission electron microscopy (TEM) examinations were prepared in cross-sectional orientation ([010] zone-axis for STO substrates) using conventional techniques of mechanical polishing and ion thinning. The ion milling was performed using a Gatan Model 691 precision ion polishing system (PIPS). The bright-field (BF) imaging, selected-area electron diffraction (SAED) and HRTEM examinations were carried out on a JEOL JEM 2100F electron microscope operated at 200 kV.

The magnetic properties were measured using a commercial superconducting quantum interference device magnetometer (SQUID, Quantum Design Company) with a temperature down to 5 K and a magnetic field up to 10 T. The transport properties were characterized by the physical property measurement system (PPMS) with a temperature down to 2 K and a magnetic field up to 13 T. The magnetic field was parallel to the sample surface as well as the current direction.

3. Results and discussion

Fig. 1(a) shows a cross-sectional BF TEM image of the unannealed LSCO/STO sample with a film thickness of 30 nm, recorded at room temperature. The BF image was taken under a two-beam condition with $\mathbf{g} = 002$. Two white arrows indicate the interface between the LSCO and STO. Just as we can see, the film is homogeneous and its surface is smooth. Fig. 1(b) shows a [010] zone-axis SAED pattern recorded from the LSCO film and it can be indexed using the pseudo-cubic unit cell ($a = 3.82$ Å). Obviously, many dots (labeled with white arrows) which should be extinct, appeared at 1/2 positions between the fundamental reflections. The wave vectors of these dots can be written as [0, 0, 1/2] and [1/2, 0, 0], which represents a modulated structure with a periodicity of two-fold the original unit lattice distance. At the same time, a typical [010] zone-axis SAED pattern recorded from the substrate (STO) is shown in Fig. 1(c). Contrary to the SAED from the film, no extra reflections can be found. To better understand these extra dots, a typical HRTEM image taken from region R_1 in Fig. 1(a) is shown in Fig. 1(d). In the HRTEM image, the alternative bright and dark stripes are clear. Based on the intensity profiles, we assure that the modulated structures exist in the LSCO film. As we all know, both La^{3+} and Sr^{2+} cations have the similar ionic radii and when Sr is doped, the charge can be balanced by the conversion of Co^{3+} into Co^{4+}. If no oxygen vacancies exist in the film before the annealing process, the ionic states of LSCO is $La^{3+}_{0.67}Sr^{2+}_{0.33}Co^{3+}_{0.67}Co^{4+}_{0.33}O^{2-}_{3}$. Therefore, the lattice substitution between La and Sr is possible. The structure model proposed in Fig. 1(f) is based on the assumption that lattice substitution between Sr and La is permitted in LSCO film [1]. In order to verify the atomic model, systematic HRTEM simulations were performed and one simulated image with $\Delta f = -60.0$ nm (defocus value) and $t = 29.9$ nm (thickness) is shown in Fig. 1(e). It is apparent that the simulated image is in good agreement with the experimental one. In B-sites, no contrast difference can be found between pure Co^{3+} planes and Co^{4+}/Co^{3+} mixed planes, which indicates that the modulated stripes in Fig. 1(e) are not resulted from the charge ordering of Co^{4+} and Co^{3+}. On the contrary, in A-sites, the pure La^{3+} planes have the stronger intensity than the La^{3+}/Sr^{2+} mixed planes. In other words, the appearance of modulated stripes in the unannealed LSCO film is derived from the cation ordering of La^{3+} and Sr^{2+}.

To further clarify the nature of the modulation, extensive examination of the vacuum-annealed LSCO films was carried out. Different from the unannealed sample, several second phases precipitated in the epitaxial LSCO film, which are marked as I, II, III, and IV in Fig. 2(a). More importantly, the modulated stripes can be found in both A-sites and B-sites in HRTEM image of the vacuum-annealed LSCO film (Fig. 2d), which is consistent with Donner's work [16]. They found

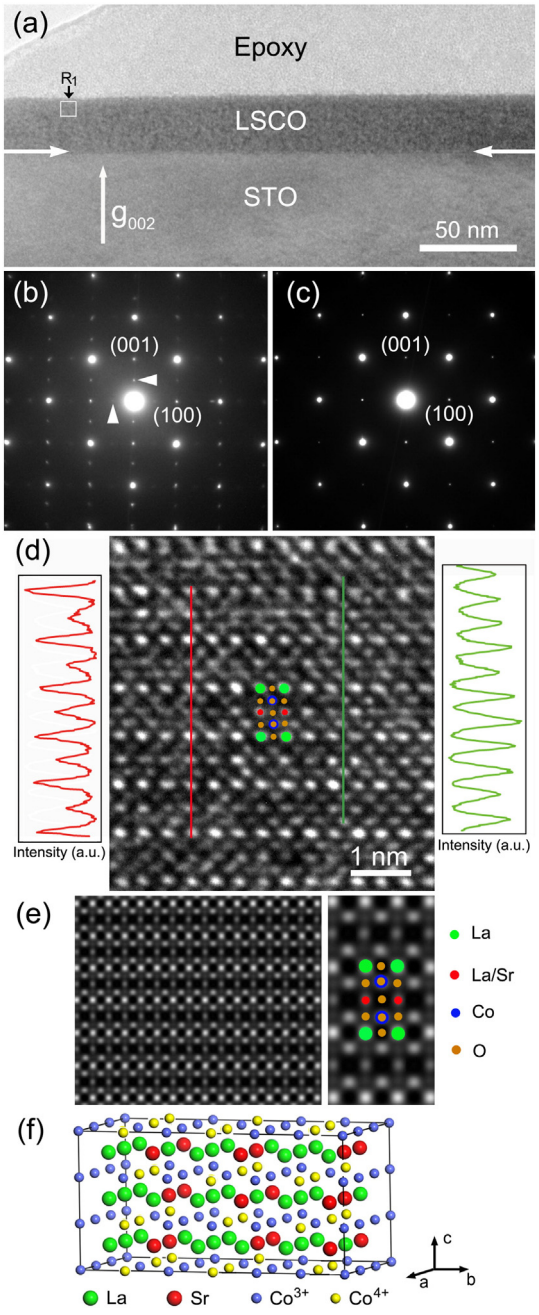

Fig. 1. (a) Cross-sectional BF image of unannealed LSCO/STO sample; (b) and (c) SAED pattern taken from the epitaxial film and the substrate, respectively; (d) Typical HRTEM image of the unannealed epitaxial LSCO film and the inset shows intensity profiles for the corresponding lines; (e) Simulated image of unannealed LSCO film with $\Delta f = -60.0$ nm and $t = 29.9$ nm and the image on the right is the magnified one; (f) Atomic model of unannealed $La_{0.67}Sr_{0.33}CoO_3$ film with oxygen atoms omitted.

that the intensity of the half-order reflection results not only from an ordering of the oxygen vacancy planes, which would only lead to a weak superstructure reflections, but also from the A-sites ordering (i.e., the difference of the form factors of La^{3+} and Sr^{2+}) by structure factor calculations. Unfortunately, they did not provide a direct evidence to support their conclusions. As we all know, oxygen vacancies were introduced when annealing the film in vacuum. If all Co^{4+} cations convert into Co^{3+}, after the annealing process, the ionic state of LSCO is $La^{3+}_{0.67}Sr^{2+}_{0.33}Co^{3+}O^{2-}_{2.835}V^{O}_{0.165}$. So it is reasonable to assume that the additional modulated stripes in vacuum-annealed LSCO film relative to unannealed film are induced by the ordering of oxygen vacancies. From the extensive experimental results before and after annealing,

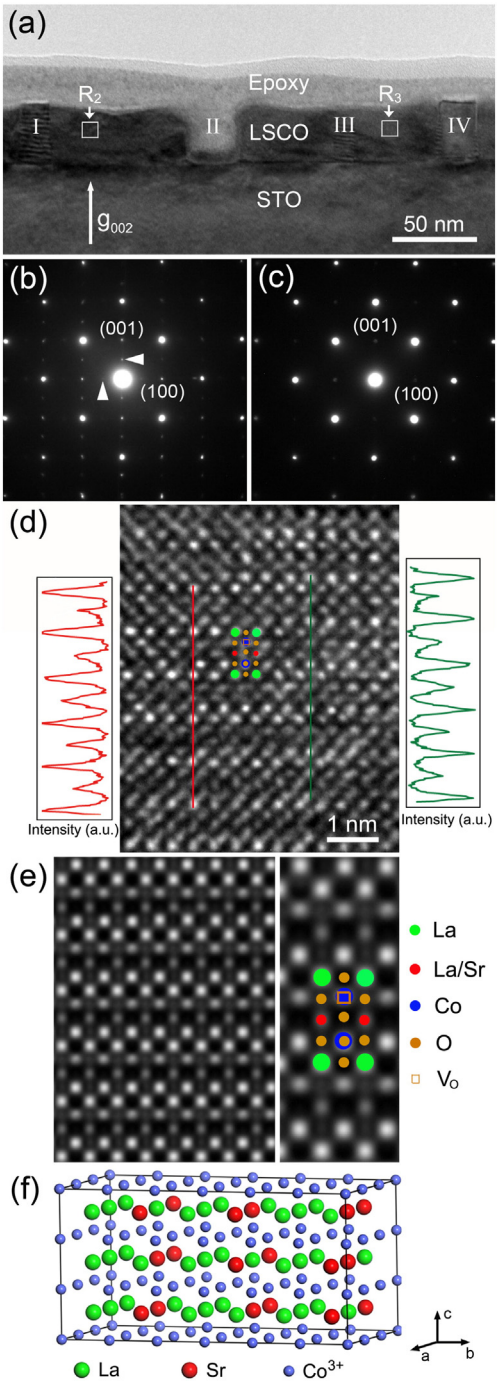

Fig. 2. (a) Cross-sectional BF image of vacuum-annealed LSCO/STO sample; (b) and (c) SAED pattern taken from the epitaxial film and the substrate, respectively; (d) Typical HRTEM image of the vacuum-annealed epitaxial LSCO film and the inset shows intensity profiles for the corresponding lines; (e) Simulated image of vacuum-annealed LSCO film with $\Delta f = -73.0$ nm and $t = 16.8$ nm and the image on the right is the magnified one; (f) Atomic model of vacuum-annealed $La_{0.67}Sr_{0.33}CoO_3$ film and oxygen atoms were also omitted.

an atomic model was proposed for the vacuum-annealed LSCO thin film, which is shown in Fig. 2(f) (oxygen atoms are omitted for clarity). To prove the validity of this atomic model, HRTEM simulations were also performed. Just like the unannealed LSCO film, La^{3+}/Sr^{2+} ions are regularly arranged and the charge is balanced by oxygen vacancy ordering. The simulated HRTEM image (Fig. 2(e)) agrees well with the experimental one. In A-sites, the intensity of pure La^{3+} planes is stronger than that of La^{3+}/Sr^{2+} mixed planes; in B-sites, the Co–O planes containing oxygen vacancies are weaker than the others. Then we proposed that the modulated structure in A-sites is caused by the cation ordering of La^{3+}/Sr^{2+} and the modulated structure in B-sites is derived from the oxygen vacancy ordering.

Fig. 3(a) is a typical HRTEM image taken from region R_3 (marked in Fig. 2(a)). Three different kinds of domain structures, i.e. no stripes region (I), vertical stripes region (II) and horizontal stripes region (III), appear in this image. The simulated HRTEM image of the vacuum-annealed LSCO film was performed along different directions. When we carry out the simulation along [100] or [001] with $\Delta f = -73.0$ nm and $t = 16.8$ nm, the modulated stripes are obvious. Unsurprisingly, no contrast difference is observed when we simulate along [010]. The simulated results (shown in Fig. 3(b), Fig. 3(c) and Fig. 3(d)) agree well with the experimental images. In other words, the atomic model satisfies the symmetry of all domains. In addition to the novel modulated structures, an anisotropic chemical expansion was also investigated in the vacuum-annealed LSCO thin film using HRTEM at room temperature. The typical HRTEM images taken from horizontal and vertical stripes regions are shown in Fig. 4(a) and Fig. 5(a), respectively. To see the details of these modulated structures, enlarged HRTEM images are also demonstrated. From the interatomic spacing between the neighboring atoms extracted from the intensity profiles, as shown in Fig. 4(c) and Fig. 5(c), respectively, we found that the lattice parameters along the direction of modulated structures (~3.91 Å) are significantly larger than those along other directions (~3.86 Å). In order to confirm the universality of this conclusion, the HRTEM image with no stripes was also investigated and the results are shown in Fig. 6. In this image, no modulated stripes can be found and the lattice parameters of both two directions are ~3.86 Å. This verified our conclusion that the anisotropic chemical expansion is larger along the direction of the modulated structure relative to the others. Properly speaking, the anisotropic chemical expansion is always vertical to the oxygen vacancy ordering planes. In the vacuum-annealed LSCO film, Co^{4+} cations were reduced into Co^{3+} and oxygen vacancies were introduced. No chemical expansion could happen if the oxygen vacancies are arranged disorderly. Thus we proposed that the anisotropic chemical expansion is derived from the oxygen vacancy ordering rather than the reduction of oxidation state of Co^{4+}, which is in discrepancy with the previous report [7].

Fig. 7 shows temperature-dependent magnetization M(T) and magnetic hysteresis loop M(H) curves of the LSCO films with H applied along the in-plane direction. In Fig. 7(a), we observed a typical paramagnetic–ferromagnetic transition in the unannealed LSCO film. As reported in the literature [17,18], the Curie temperature of LSCO is ~200 K. Similarly, the M(H) curve for unannealed LSCO in Fig. 7(b) also shows a clear ferromagnetic hysteresis loops with similar coercive fields. In contrast, the vacuum-annealed LSCO films do not show any discernible magnetic transition or hysteresis loop. As we all know, LSCO exhibits ferromagnetism through double-exchange interaction between the Co–O–Co bonds. In the vacuum-annealed LSCO film, the oxygen vacancies were introduced, which could destroy the double-exchange interaction between the Co–O–Co bonds and introduce a frustration into the magnetically coupled network that presumably leads to a spin-glass magnetic state. In other words, the ferromagnetism disappeared due to the introduction of oxygen vacancies.

In addition to the magnetism, the transport properties of the film are also investigated. Fig. 8 shows the temperature-dependent resistance (R–T) of vacuum-annealed (red curve) and unannealed (black curve) LSCO films. The resistance of the unannealed LSCO film increases with the temperature, which is characteristic for metals. Whereas in the vacuum-annealed LSCO thin film, the R–T curve exhibits a typical insulator feature. This means that a metal-insulator transition occurs when annealing the LSCO film in vacuum. Like the ferromagnetism, the conductivity is being strongly affected by the introduction of oxygen vacancies into the lattice [19]. After annealing in the vacuum, Co^{4+} cations were reduced into Co^{3+} and oxygen vacancies were introduced. Due

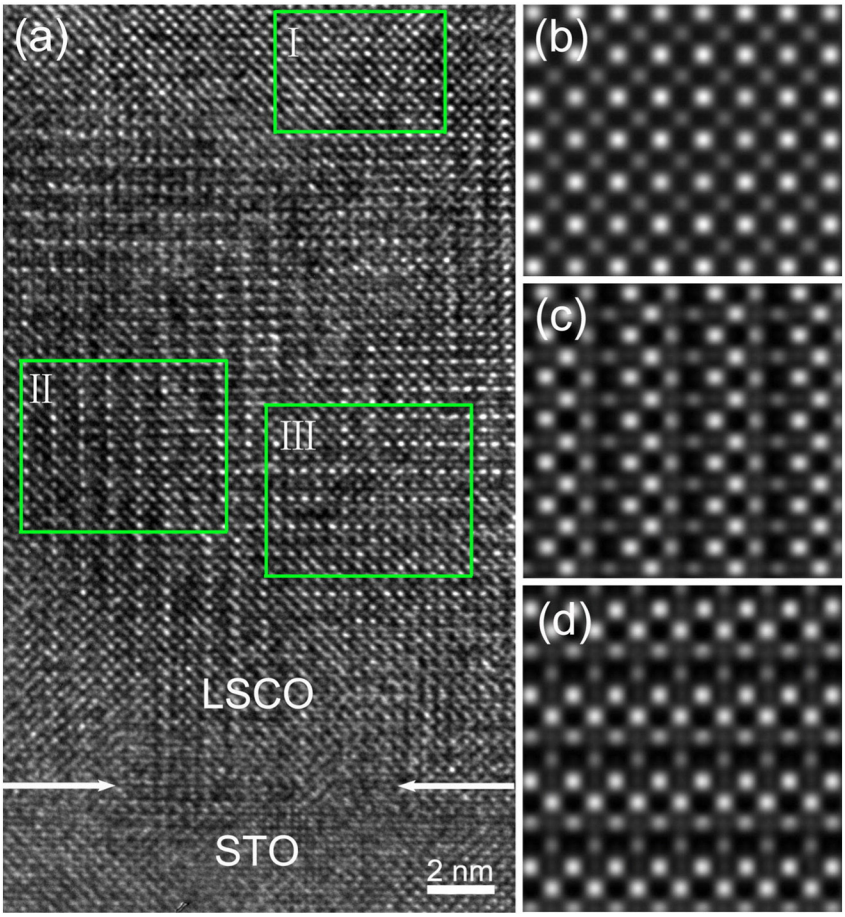

Fig. 3. (a) Typical HRTEM image of the vacuum-annealed LSCO/STO sample (taken from region R_3 in Fig. 2(a)). Three kinds of domain structures are marked as I, II, III; (b) Simulated image along [010] with $\Delta f = -50.0$ nm and $t = 40.3$ nm. (c) and (d) Simulated images along [100, 001], respectively, with $\Delta f = -73.0$ nm and $t = 16.8$ nm.

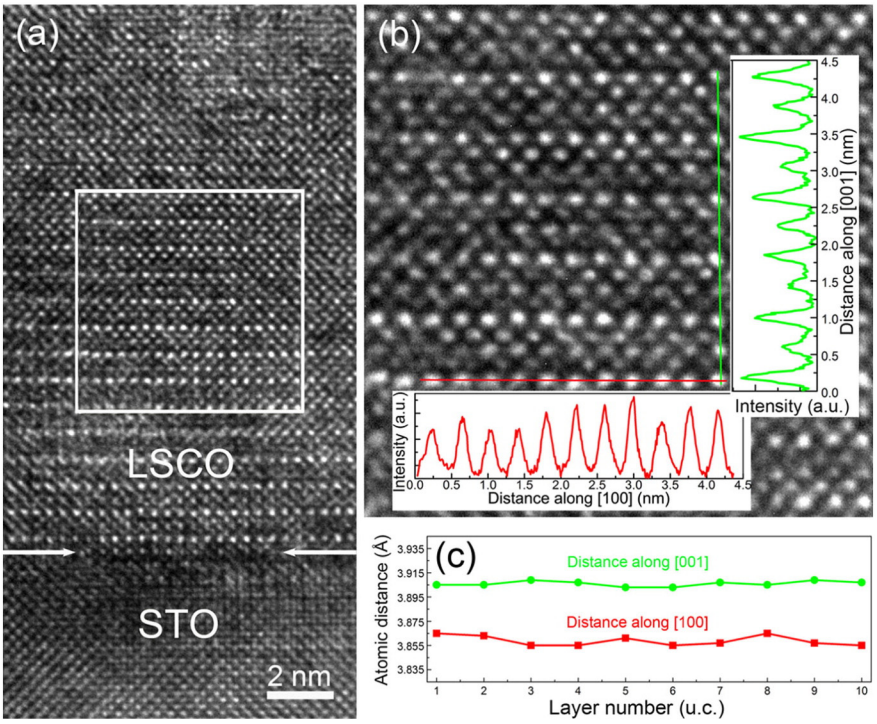

Fig. 4. (a) Typical HRTEM image of LSCO/STO film; (b) Enlarged HRTEM image marked in (a). The inset shows intensity profiles for the corresponding lines; (c) Atomic distances between A-sites atoms extracted from the insets.

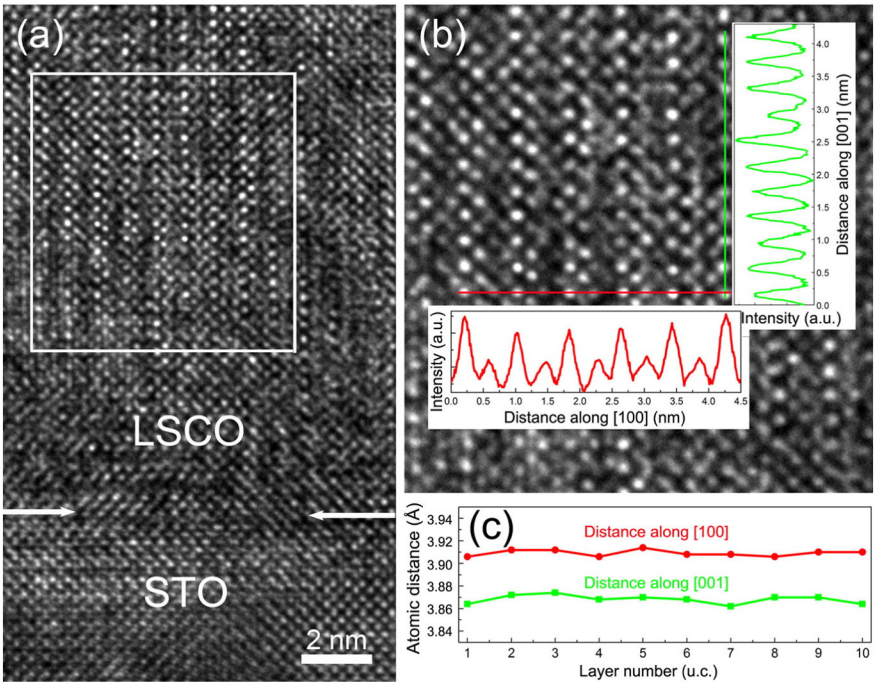

Fig. 5. (a) Typical HRTEM image of LSCO/STO film; (b) Enlarged HRTEM image marked in (a). The inset shows intensity profiles for the corresponding lines; (c) Atomic distances between A-sites atoms extracted from the insets.

to the ordering of oxygen vacancies, the double-exchange interactions were destroyed [20,21], which leads to the transformation from the ferromagnetic-metallic into a non-magnetic insulator.

4. Conclusion

Only one type of modulated structure in A-sites is observed in the unannealed LSCO thin film, while two types of modulated structures, one in A-sites and the other in B-sites, are found in the vacuum-annealed LSCO thin film. The modulated structure in A-sites is induced by the cation ordering (La^{3+} and Sr^{2+}) and the modulated structure in B-sites is derived from the oxygen vacancy ordering. In addition, it is found that the lattice expansion along the *c*-axis was significantly larger than those along *a*-axis in the vacuum-annealed LSCO thin film, which is attributed to oxygen vacancy ordering after the annealing process. The annealing process transforms the ferromagnetic–metallic LSCO film into a non-magnetic insulator due to the destruction of double-exchange interaction between the Co–O–Co bonds by the oxygen vacancy ordering.

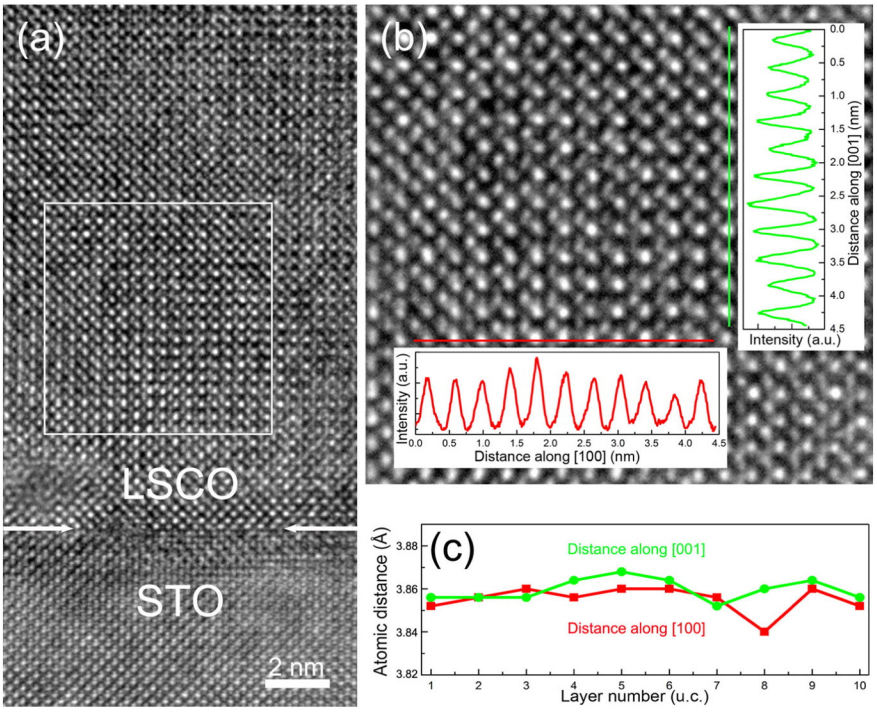

Fig. 6. (a) Typical HRTEM image of LSCO/STO film; (b) Enlarged HRTEM image marked in (a). The inset shows intensity profiles for the corresponding lines; (c) Atomic distances between A-sites atoms extracted from the insets.

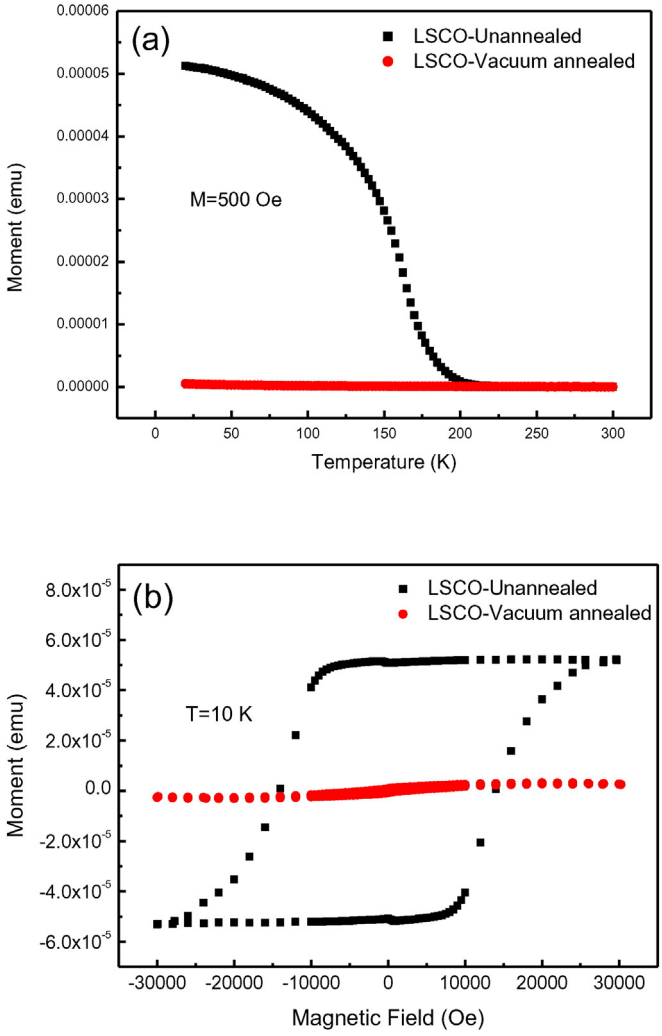

Fig. 7. Oxygen vacancy dependent magnetic properties. (a) M(T) and (b) M(H) curves for annealed (red curve) and unannealed (black curve) LSCO/STO sample. (For interpretation of the references to color in this figure legend, the reader is referred to the web version of this article.)

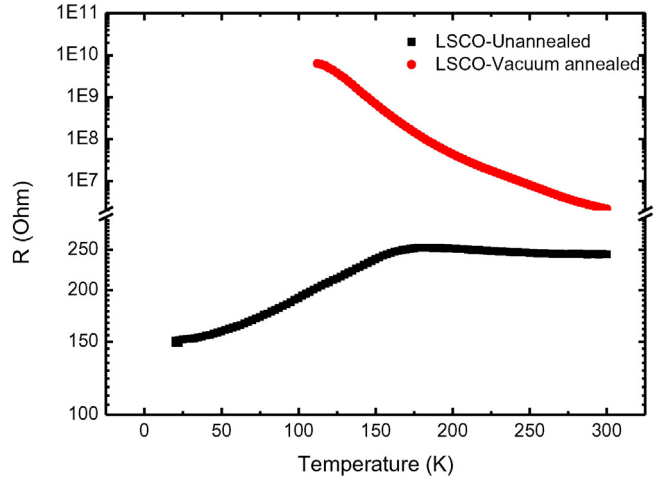

Fig. 8. The temperature dependence of the resistance for normal and vacuum annealed LSCO thin film. (For interpretation of the references to color in this figure legend, the reader is referred to the web version of this article.)

Acknowledgments

The authors would like to thank the financial support from the National Key Basic Research Development Program of China (Grant no.: 2012CB722705), the Natural Science Foundation for Outstanding Young Scientists in Shandong Province, China (Grant no.: JQ201002), and the Program for Foreign Cultural and Educational Experts (Grant nos.: W20123702083, GDW20123702162). Y.Q. Wang would also like to thank the financial support from the Top-notch Innovative Talent Program of Qingdao City (Grant no.: 13-CX-8), and the Taishan Scholar Program of Shandong Province, China.

References

[1] Z.L. Wang, Tetragonal domain structure and magnetoresistance of $La_{1-x}Sr_xCoO_3$, Phys. Rev. B 54 (1996) 1153–1158.
[2] J.H. Kwon, W.S. Choi, Y.K. Kwon, R. Jung, J.M. Zuo, H.N. Lee, M. Kim, Nanoscale spin-state ordering in $LaCoO_3$ epitaxial thin films, Chem. Mater. 26 (2014) 2496–2501.
[3] W.S. Choi, J.H. Kwon, H. Jeen, J.E.H. Borrero, A. Radi, S. Macke, R. Sutarto, F. He, G.A. Sawatzky, V. Hinkov, M. Kim, H.N. Lee, Strain-induced spin states in atomically ordered cobaltites, Nano Lett. 12 (2012) 4966–4970.
[4] J. Gazquez, W.D. Luo, M.P. Oxley, M. Prange, M.A. Torija, M. Sharma, C. Leighton, S.T. Pantelides, S.J. Pennycook, M. Varela, Atomic-resolution imaging of spin-state superlattices in nanopockets within cobaltite thin films, Nano Lett. 11 (2011) 973–976.
[5] Y.M. Kim, J. He, M.D. Biegalski, H. Ambaye, V. Lauter, H.M. Christen, S.T. Pantelides, S.J. Pennycook, S.V. Kalinin, A.Y. Borisevich, Probing oxygen vacancy concentration and homogeneity in solid-oxide fuel-cell cathode materials on the subunit-cell level, Nat. Mater. 11 (2012) 888–894.
[6] N. Biškup, J. Salafranca, V. Mehta, M.P. Oxley, Y. Suzuki, S.J. Pennycook, S.T. Pantelides, M. Varela, Insulating ferromagnetic $LaCoO_{3-\delta}$ films: a phase induced by ordering of oxygen vacancies, Phys. Rev. Lett. 112 (2014) 087202.
[7] X.Z. Chen, T. Grande, Anisotropic chemical expansion of $La_{1-x}Sr_xCoO_{3-\delta}$, Chem. Mater. 25 (2013) 927–934.
[8] V. Oygarden, T. Grande, Crystal structure, electrical conductivity and thermal expansion of Ni and Nb co-doped $LaCoO_3$, Dalton Trans. 8 (2013) 2704–2715.
[9] J. Mastin, M.A. Einarsrud, T. Grande, Structural and thermal properties of $La_{1-x}Sr_xCoO_{3-\delta}$, Chem. Mater. 18 (2006) 6047–6053.
[10] J. Mastin, M.A. Einarsrud, T. Grande, Crystal structure and thermal properties of $La_{1-x}Ca_xCoO_{3-\delta}$ ($0 \le x \le 0.4$), Chem. Mater. 18 (2006) 1680–1687.
[11] T. Grande, J.R. Tolchard, S.M. Selbach, Anisotropic thermal and chemical expansion in Sr-substituted $LaMnO_{3+\delta}$: implications for chemical strain relaxation, Chem. Mater. 24 (2012) 338–345.
[12] M.A. Torija, M. Sharma, M.R. Fitzsimmons, M. Varela, C. Leighton, Epitaxial $La_{0.5}Sr_{0.5}CoO_3$ thin films: structure, magnetism, and transport, J. Appl. Phys. 104 (2008), 023901.
[13] D. Phelan, S. Rosenkranz, S.H. Lee, Y. Qiu, P.J. Chupas, R. Osborn, H. Zheng, J.F. Mitchell, J.R.D. Copley, J.L. Sarrao, Y. Moritomo, Nanomagnetic droplets and implications to orbital ordering in $La_{1-x}Sr_xCoO_3$, Phys. Rev. Lett. 96 (2006), 027201.
[14] Q.M. Zhang, Q. Li, R.L. Gao, W.P. Zhou, L.Y. Wang, Y.T. Yang, D.H. Wang, L.Y. Lv, Y.W. Du, The electric field manipulation of magnetization in $La_{1-x}Sr_xCoO_3/Pb(Mg_{1/3}Nb_{2/3})O_3$–$PbTiO_3$ heterostructures, Appl. Phys. Lett. 104 (2014), 142409.
[15] Z. Hu, C. Grazioli, M. Knupfer, M.S. Golden, J. Fink, P. Mahadevan, A. Kumar, S. Ray, D.D. Sarma, S.A. Warda, D. Reinen, S. Kawasaki, M. Takano, C. Schussler-Langeheine, C. Mazumdar, G. Kaindl, Difference in spin state and covalence between $La_{1-x}Sr_xCoO_3$ and $La_{2-x}Sr_xLi_{0.5}Co_{0.5}O_4$, J. Alloy. Compd. 343 (2002) 5–13.
[16] W. Donner, C.L. Chen, M. Liu, A.J. Jacobson, Y.L. Lee, M. Gadre, D. Morgan, Epitaxial strain-induced chemical ordering in $La_{0.5}Sr_{0.5}CoO_{3-\delta}$ films on $SrTiO_3$, Chem. Mater. 23 (2011) 984–988.
[17] Y.J. Yoo, K.K. Yu, J.Y. Kim, Y.P. Lee, K.W. Kim, K.P. Hong, Physical properties of $La_{1-x}Sr_xCoO_3$, Phys. B Condens. Matter 385 (2006) 411–414.
[18] Z. Othmena, A. Schulman, K. Daoudia, M. Boudard, C. Acha, H. Roussel, M. Oueslatia, T. Tsuchiya, Structural, electrical and magnetic properties of epitaxial $La_{0.7}Sr_{0.3}CoO_3$ thin films grown on $SrTiO_3$ and $LaAlO_3$ substrates, Appl. Surf. Sci. 306 (2014) 60–65.
[19] X.G. Chen, J.B. Fu, C. Yun, H. Zhao, Y.B. Yang, H.L. Du, J.Z. Han, C.S. Wang, S.Q. Liu, Y. Zhang, Y.C. Yang, J.B. Yang, Magnetic and transport properties of cobalt doped $La_{0.7}Sr_{0.3}MnO_3$, J. Appl. Phys. 116 (2014) 103907.
[20] J.R. Sun, C.F. Yeung, K. Zhao, Strain-dependent vacuum annealing effects in $La_{0.67}Ca_{0.33}MnO_{3-\delta}$ films, Appl. Phys. Lett. 9 (2000) 1164–1166.
[21] J.R. Sun, H.W. Yeung, H. Li, K. Zhao, H.N. Chan, H.K. Wong, Oxygen content dependence of the transport property of $La_{2/3}Sr_{1/3}CoO_{3-\delta}$ film, J. Appl. Phys. 90 (2001) 2831–2835.